Proceedings of the ASME 2012 31st International Conference on Ocean, Offshore and Arctic Engineering
OMAE2012
July 1-6, 2012, Rio de Janeiro

OMAE2012-83757

LOADS FROM CURRENTS AND WAVES ON NET STRUCTURES

Are Johan Berstad
Dr. Ing. Aquastructures www.aquastructures.no,
Email: are.berstad@aquastructures.no

Jørgen Walaunet
M.Sc..Aquastructures www.aquastructures.no,
Email: jw@aquastructures.no

Line Fludal Heimstad
M.Sc. NTNU lineflud@stud.ntnu.no

ABSTRACT
The aquaculture industry has increased rapidly the last 20 years. In almost all fish farms, the fish is held captured in net cages. Net structures are built up with twines as shown in Figure 1.
Various parameters of importance for the loads to nets such as solidity, Reynolds number, flow angle relative to mesh and increased flow around twines compared to single twines. This paper outlines such effects.
This paper consider loads to net panels considering the net a sum of twines and then sum the forces twine by twine. Based on this approach the paper presents a calculation method for net meshes. The presented load formulation is valid for rectangular and diamond shaped meshes and is valid for any 3D orientation of flow relative to mesh.
The presented method for load calculation includes methodology for deriving the forces to a net structure based on knowledge of drag resistance for an individual twine. This methodology is compared with other published formulae and empirical data.
A formula is presented based on a twine in wake consideration. The presented formula is compared to measurements for test cases both in terms of a net panel and for a full cage model. Results show good agreement.

INTRODUCTION
The revised Norwegian Standard, NS 9415 (2009) have refined design criteria for nets used in fish farming in Norway. As stated now all net cages meeting one of the below criteria must have its capacity validated through analysis:

- Net depth larger than 40 meters
- Net circumference larger than 170 meters
- 50 year wave height (Hs) larger than 2.5 meters.
- 50 year current velocity larger than 0.75 meters.

Figure 1 Typical net structure.

Several efforts have been carried out on loads to net membranes, among them are Fredheim (2005), Tsukrov et al (2003), Lader et al (2007, 2008) This paper focus on the load formulation used in and applicable for the FE analysis program, AquaSim (Aquastructures 2006, Berstad et. al. 2004). The AquaSim analysis tool most commonly used for calculations of loads and response in fish farms today. Prior to NS 9415(2009) analysis of nets has mostly been as part of models with the aim of design and dimensioning of fish farm moorings, cages or barges.
The program utilizes a corotated FE formulation. Loads from waves and currents are applied accounting for structural deflection, denoted hydroelastic analysis. Hence fish farms which are systems with combination of stiff and soft parts can be analysed as an integrated coupled system.

The basic AquaSim net mesh model is a twine by twine model. This paper presents a refined net mesh load model. This new model has been introduced to AquaSim and is compared to the basic load model and empirical data.

DEFINITIONS AND ASSUMPTIONS
Much work has been carried out on 2D cross-flow around cylinders. A possible flow pattern around a circular cylinder is shown in Figure 2. As seen from this figure, the cylinder introduces a disturbance to the flow in the wake.

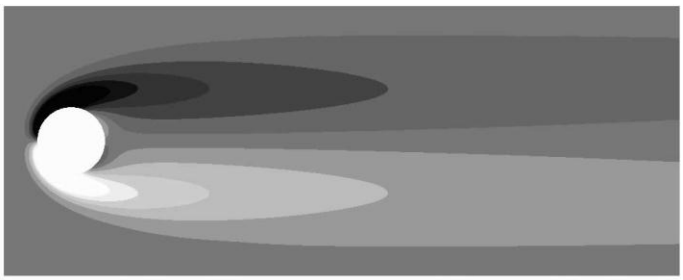

Figure 2 Example of 2D flow around a cylinder. From Barkley(2006). The colours indicated vorticity by greyscale.

In accordance with Lord Rayleigh (Morison et al 1950), the force for steady flow acting on the cylinder is expressed as:

$$F = Cd_{cyl}\frac{\rho}{2}dLv^2 \quad (1)$$

where F is the drag force, Cd_{cyl} is the drag coefficient for cross flow to a circular cylinder, ρ is the density of water, L is the length of the cylinder, d is the diameter of the cylinder and v is the fluid velocity. In 3D, the velocity in Equation (1) can be interpreted as the cross flow velocity which is the velocity in the plane of the cylinder cross section.

Consider flow in the direction perpendicular to the plane of the mesh in Figure 1. Define a coordinate system where the net is located in the *y-z* plane and the flow direction is along the positive *x*- axis. The difference between a single twine and a net is that water flowing through the mesh must pass not only a twine or cylinder, but several twines as seen in Figure 3.

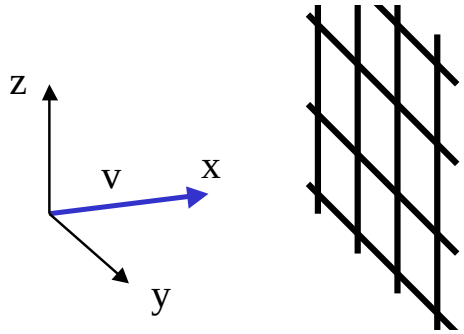

Figure 3 Flow perpendicular to net

The most important parameter used to describe nets is the term solidity (*Sn*). Several definitions are applied to this term. The most common formal definition is $Sn = A_e / A_{tot}$, where A_e is the area casting shadow from a light perpendicular to the net and A_{tot} is the total area of the net.

Consider an excerpt of a net seen in Figure 4.

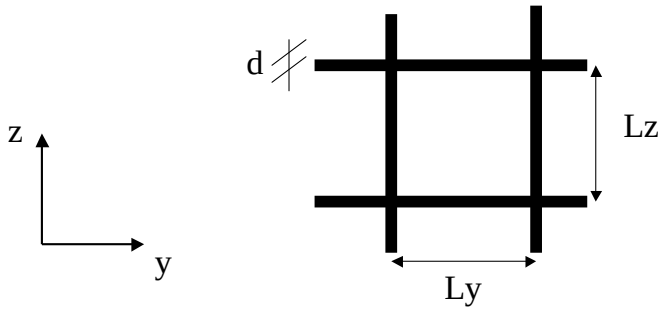

Figure 4 Basic definition for a net.

For an ideal knotless mesh as shown in Figure 4 a mathematical expression for *Sn* can be formulated as:

$$Sn = \frac{d}{Ly} + \frac{d}{Lz} - \frac{2d^2}{Ly^2 + Lz^2} \quad (2)$$

Other definitions have been applied. Historically meshes were made with knots. This leads to higher solidity. A term having been used by e.g Løland (1991) is:

$$Sn_{kn} = \frac{d}{L_y} + \frac{d}{L_z} + \frac{kd^2}{2(L_y^{\,2} + L_z^{\,2})} \quad (3)$$

where k is a constant typically 1 or 2. Yet another simplified definition is:

$$Sn_{2d} = \frac{d}{L_y} + \frac{d}{L_z} \quad (4)$$

This is often denoted the "2D solidity" since it basically is based on summing diameters in both directions. Knotless nets are sown as shown in Figure 1, meaning the net will not be "mathematically perfect". Hence the 2D solidity can be a realistic definition of solidity.

Using the twine by twine method, the drag force can be found as:

$$F = Cd\frac{\rho}{2}\left(\frac{d}{L_y} + \frac{d}{L_z}\right)Av^2 \quad (5)$$

where:

$$A = Lm_y \times Lm_z \quad (6)$$

for a rectangular mesh in the *y-z* plane. Note that *Cd* is not necessarily the same as Cd_{cyl}.. Lm_y is the length of the mesh in the y- direction and Lm_z is the length along the *z*- axis. The flow is along the *x*- axis.

PROPOSED RELATIONS BETWEEN Cd FOR A MEMBRANE BASED ON KNOWING THE Cd FOR AN INDIVIDUAL TWINE FROM LITTERATURE

Comparing the net seen in Figure 3 to a single line, the net will cause the flow velocity to increase due to its presence. This is in order to conserve momentum. This effect has been assessed among others in Blevins (1984). Using the undisturbed velocity, v as input in the drag equation will lead to an increased *Cd*. With origin back to Darcy (1856) and with reference to Blevins (1984) both Balash et al (2009) and Molin (2011) presents the following equation for flow perpendicular to the mesh:

$$Cd_{B1} = Cd_{cyl}\frac{Sn}{(1-Sn)^2} \quad (7)$$

where Cd_{B1} refers to an adjusted *Cd* relative to Cd_{cyl} which would be the corresponding *Cd* for a single twine. An adjusted formulation also originating back to Blevins (1984) propose

$$Cd_{B2} = Cd_{cyl}\frac{\beta Sn(2-Sn)}{(1-Sn)^2} \quad (8)$$

where β is a tabulated value. Kristiansen and Faltinsen (2011) introduce 0.5 to the above equation:

$$Cd_{KF} = Cd_{cyl}\frac{Sn(2-Sn)}{2(1-Sn)^2} \quad (9)$$

In the above formulae the drag coefficient, *Cd* is expressed in terms of the solidity, *Sn*. This means that all formulae will depend on the definition of *Sn*.

AN ANALYTIC APPROACH TO ESTABLISHMENT OF *Cd* FOR A NET BASED ON KNOWING THE *Cd* FOR AN INDIVIDUAL TWINE (Cd_{cyl})

This paper introduces an alternative relation between Cd_{cyl} and Cd_{mem} than presented by other authors in Equation (7-9).

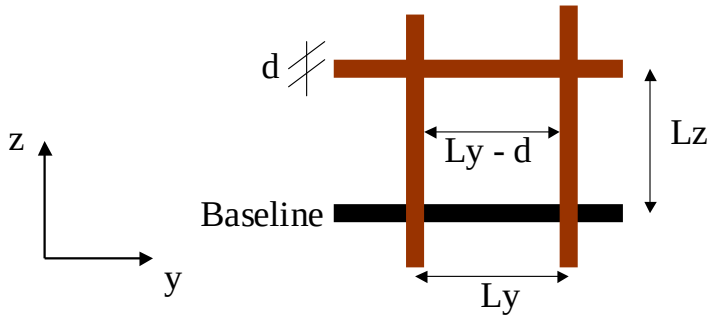

Figure 5 One twine denoted as baseline

Consider the lower horizontal line in Figure 5. The flow (along the x- axis) can only pass this twine in parts of the twine where there is no crossing twine. This leads to an effective length of the twine, Ly_{eff} of:

$$Ly_{eff} = Ly - d \quad (10)$$

Because the flow must pass through a cross flow area smaller than the full area of the flow, the flow velocity must increase in order keep the momentum of the flow. With reference to Figure 5 one can see that the velocity passing the mesh, v_{eff}, must be increased to

$$v_{eff} = \frac{vLyLz}{(Ly-d)(Lz-d)} \quad (11)$$

Introducing Ly_{eff} and v_{eff} to Equation (1),

$$F = Cd\frac{\rho}{2}Ly_{eff}\,dv_{eff}^{\ 2} \quad (12)$$

gives:

$$F = Cd\frac{\rho}{2}(Ly-d)d\left(\frac{vLyLz}{(Ly-d)(Lz-d)}\right)^2 \quad (13)$$

which rearranged gives this relation:

$$F = Cd\frac{\rho}{2}dL_y v^2\frac{L_y L_z^{\ 2}}{(L_y-d)(L_z-d)^2} \quad (14)$$

This can be expressed as:

$$F = Cd_{mem}\frac{\rho}{2}dL_y v^2 \quad (15)$$

where:

$$Cd_{mem} = Cd_{cyl}\frac{L_y L_z^{\ 2}}{(L_y-d)(L_z-d)^2} \quad (16)$$

Introducing $Ly = Lz = L$

$$Cd_{mem} = Cd_{cyl}\frac{1}{(1-\frac{d}{L})^3} \quad (17)$$

Introducing *Sn2D* as *Sn* in the above equation gives:

$$Cd_{mem} = Cd_{cyl}\frac{1}{(1-\frac{Sn}{2})^3} \quad (18)$$

which is in a form easily comparable to the expressions seen in Equation (7-9). By comparing these it is seen that the above equation has a different form.

As an alternative way to view Figure 5 one may consider only velocity reduction from adjacent twines not including the twine being the considered as the circular cross section itself. In this case the effective difference in velocity (v_{eff}) between one twine and a net may be expressed as:

$$v_{eff} = \frac{VLyLz}{(Ly-d)(Lz-d/2)} \quad (19)$$

Introducing Ly_{eff} and v_{eff} to Equation (1) gives:

$$F = Cd\frac{\rho}{2}(Ly-d)d\left(\frac{vLyLz}{(Ly-d)(Lz-d/2)}\right)^2 \quad (20)$$

which rearranged gives this relation:

$$F = Cd\frac{\rho}{2}dL_y v^2\frac{L_y L_z^{\ 2}}{(L_y-d)(L_z-d/2)^2} \quad (21)$$

In this case the *Cd* for the membrane is denoted Cd_{mem_v2} where:

$$F = Cd_{mem\_v2}\frac{\rho}{2}dL_y v^2 \quad (22)$$

where:

$$Cd_{mem\_v2} = Cd_{cyl}\frac{L_y L_z^{\ 2}}{(L_y-d)(L_z-d/2)^2} \quad (23)$$

Introducing $Ly = Lz$

$$Cd_{mem\_v2} = Cd_{cyl}\frac{1}{(1-\frac{d}{L})(1-\frac{d}{2L})^2} \quad (24)$$

Introducing *Sn2D* as a simplification to Sn gives:

$$Cd_{mem\_v2} = Cd_{cyl}\frac{1}{(1-\frac{Sn}{2})(1-\frac{Sn}{4})^2} \quad (25)$$

Neglecting higher order terms in Sn this gives:

$$Cd_{mem\_v2\_simp} = Cd_{cyl} \frac{1}{(1-\frac{Sn}{2})^2} \quad (26)$$

which is in a form easily comparable to the expressions seen in Equation (7-9).

A third version of Cd_{mem}, Cd_{mem_v3} may be outlined by applying the velocity correction without accounting for the reduced effective length of each twine. This will give the following expression for Cd_{mem_v3}:

$$Cd_{mem\_v3} = Cd_{cyl} \frac{L_y L_z^{\,2}}{(L_y - d)^2 (L_z - d)^2} \quad (27)$$

Introducing $Ly = Lz$

$$Cd_{mem\_v3} = Cd_{cyl} \frac{1}{(1-\frac{d}{L})^4} \quad (28)$$

Introducing Sn_{2D} as a simplification to Sn gives:

$$Cd_{mem\_v3} = Cd_{cyl} \frac{1}{(1-\frac{Sn}{2})^4} \quad (29)$$

Figure 6 shows a comparison on 5 of the above equations. The Sn_{2D} equation is used as the expression linking solidity and diameter.

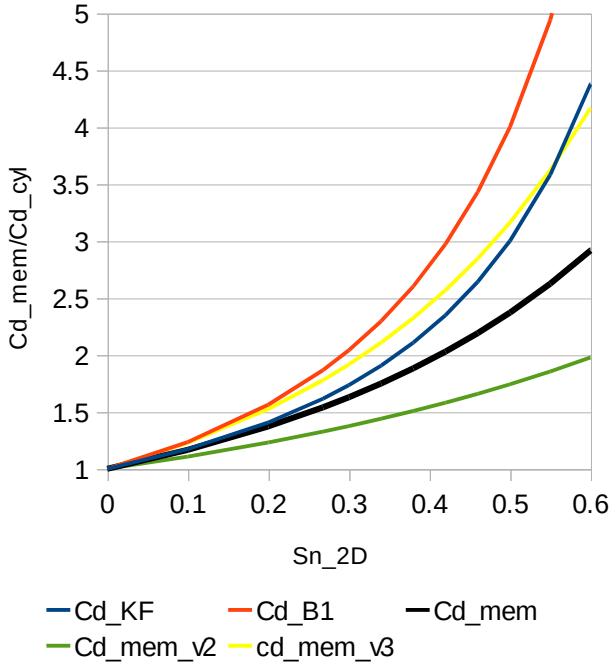

Figure 6 Comparison of difference expressions for accounting for the increased velocities from mesh effects.

As seen from Figure 6 there is a large increase in drag coefficient by increasing the solidity.

Comparing the 5 different alternatives for drag increase from increased solidity it is seen that Cd_{mem_v3} and Cd_{B1} and Cd_{KF} are in the similar range while Cd_{mem} has less increase from increased solidity while Cd_{mem_v2} is the lowest curve. Based on the analytic consideration outlined in this paper, Cd_{mem} and Cd_{mem_v2} are chosen as being the two curves explained best analytically. Since Cd_{mem} is seen to be closest to alternative formulations, Cd_{mem} is the equation introduced to the Aquasim software and compared to empirical results.

Having established a relation between Cd_{cyl} applicable for a single twine and Cd_{mem} applicable for the mesh as seen in Figure 6, the next section describes how Cd_{cyl} is established.

ESTABLISHING Cd_{cyl} FOR AN INDIVIDUAL TWINE

Much study has been carried out on drag coefficients on circular cylinders with an example of an established relation shown in Figure 7. Drag coefficients is typically a function of Reynolds number, Rn, where:

$$Rn = \frac{vd}{\nu} \quad (30)$$

where ν is the kinematic viscosity of the fluid. ν is in order of magnitude 10^{-6} [m2/s] for salt water. For a typical net, diameter, d is around 1 mm and a typical design value for current velocity, v is around 1 m/s. In this case Rn will be in order of magnitude 10^3. This will give a drag coefficient a little less than 1 according to Figure 7.

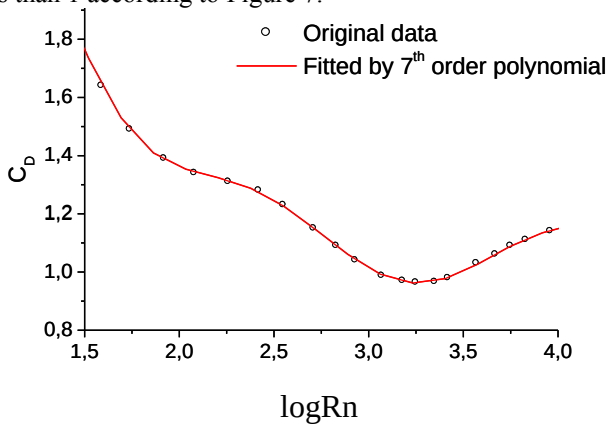

Figure 7 Drag coefficient, Cd_{cyl}, as function of Reynolds number, Rn (Goldstein 1965).

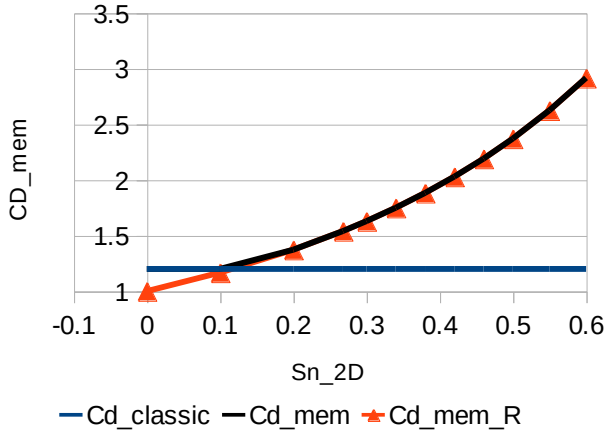

Figure 8 Alternatives for Cd implemented in Aquasim

Cd_classic refers to a model where $Cd_{mem} = 1.2$, independent of Rn and Sn, meaning it is not increased for the effect shown in Figure 6.

The new refined net mesh models give the user the possibility to find Cd_{cyl} based on Rn,. Then the input Cd_{cyl} is multiplied with Cd_{mem}/Cd_{cyl} as seen in Figure 6 to establish Cd_{mem_R} for use in the analysis.
The black line in Figure 8 shows the alternative option to establish Cd_{mem}. In this case Cd_{cyl} = 1 and Cd_{mem} is max (1.2, Cd_{mem} as seen in Figure 8).

FORCES ON TWINES FROM FLUID VELOCITY AT AN ARBITRATY ANGLE.

The above considerations have been based on flow normal to the net. In general the relative fluid velocity, v, to the net and each twine can be in any direction as shown in Figure 9.

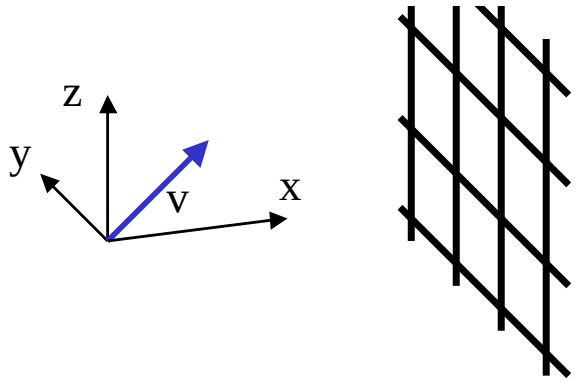

Figure 9 Mesh with fluid velocity in an arbitrary direction relative to net.

Considering a single twine, the flow can be at any direction relative to the twine as shown in Figure 10. The velocity, v is decomposed to a component normal to the plane v_n and a component tangential to the twine v_t. A basic assumption in the load model is that the resulting force is in the plane of v_n and v_t.

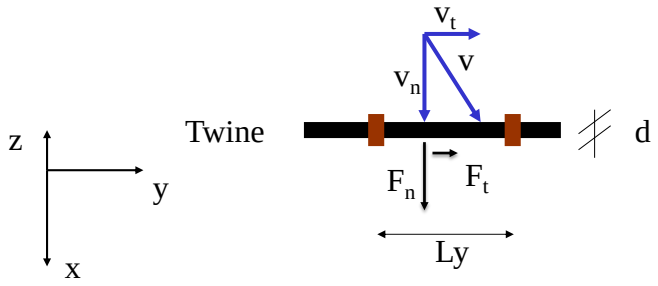

Figure 10 Velocity inflow to a twine

Applying the cross flow principle, the load normal to the twine, F_n is found as:

$$F_n = Cd_{mem}\frac{\rho}{2}dLv_n^{\,2} \qquad (31)$$

whereas the force in tangential to the twine is derived as:

$$F_t = Ct\frac{\rho}{2}\pi dLv_t^{\,2} \qquad (32)$$

where Ct normally is in the range of 1-2% of Cd. The inflow velocity v is the relative velocity to the twine and is found as:

$$v = v_c + v_w - v_m \qquad (33)$$

where v_c is the current velocity, v_w is the fluid velocity introduced by the wave motions and v_m is the velocity of the mesh.
As seen from the above consideration, lift forces introduced to the net are due to the cross flow lift effect on individual twines.

DRAG FORCES TO NET WHEN FLOW IN LINE WITH MESH PLANE

Consider a case with a net in the y-z plane as shown in Figure 11. Empirical results for a wide range of nets have shown that calculating forces to the net based on the twine by twine method without accounting for shadow effects due to twines located "on the wheel" of each other will lead to largely conservative results (e.g. Blevins 1984, Løland 1991, SFH 2010, Kristiansen and Faltinsen 2011). Empirical results show that this effect normally occurs when the angle Φ as defined in Figure 11 passes 45-60°
In Figure 11 it is the twines in the z- direction that are on the wheel of each other relative to the flow direction which is along the y- direction.

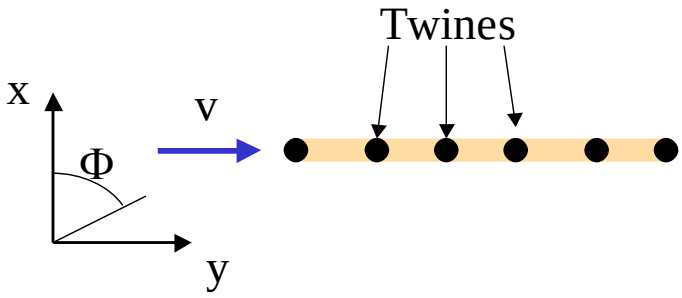

Figure 11 Flow in line with mesh

This paper presents a correction for the "on the wheel" effect for flow angles at a certain angle, Φ to the mesh.
Consider a case with an arbitrary flow angle to the mesh. As in Figure 11 define the cross flow. The cross flow with respect to the twines in the z- direction, v_n is in the x-y plane at an angle Φ to the mesh as defined in Figure 12.

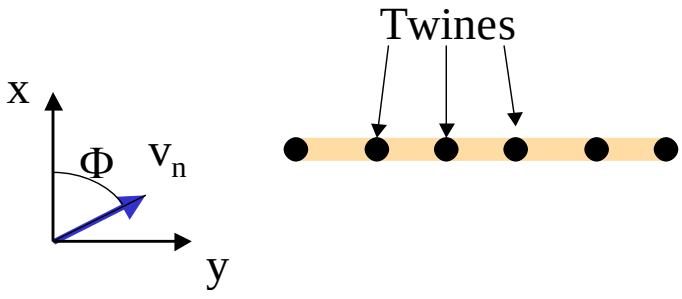

Figure 12 Cross flow velocity at angle Φ to z- directed twines in the mesh.

Consider a twine assuming the shape of a cylinder. The flow passing though the twine will generate a wake with a disturbed flow field. Figure 13 shows a twine located in the wake of an upstream twine. This resembles the case as it is for a net as seen in Figure 12.

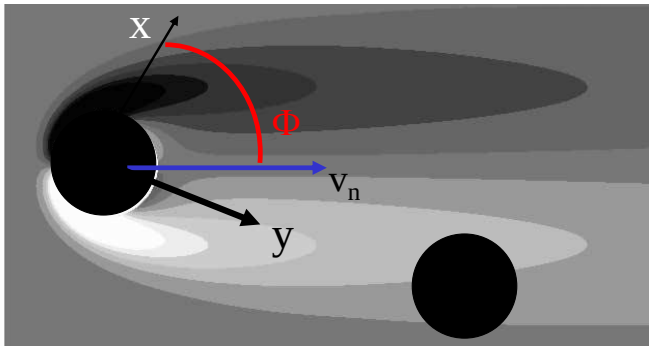

Figure 13 Twine located in wake of former twine

The shape of the wake seen in Figure 13 depends on the Reynolds number. The case seen in Figure 2 and Figure 13 is for low Reynolds number < 40. Figure 14 shows the constant but unstable baseflow at *Re* =100 whereas Figure 15 shows a snapshot of the vortex shedding behind a cylinder. Figures are from Barkley (2006).

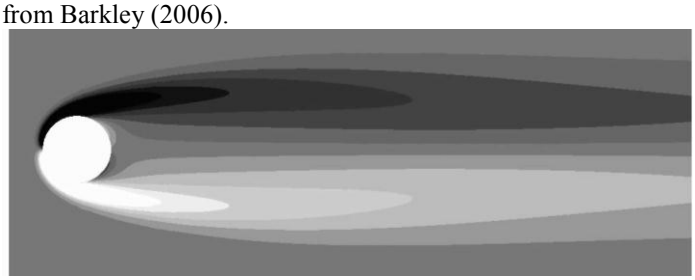

Figure 14 y- Constant but unstable baseflow at Re = 100

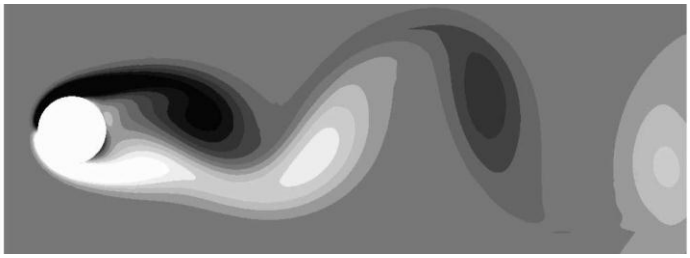

Figure 15 Vortex shedding at Re = 100

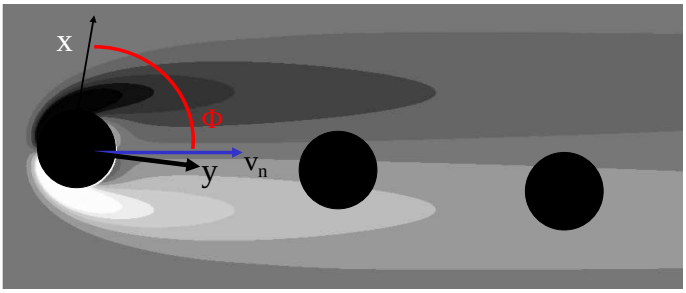

Figure 16 Flow angle close to 90°.

As well known, and seen from Figure 2, Figure 14 and Figure 15 flow passing a cylinder will give a perturbation in the velocity field behind the cylinder. As seen from these figures the flow area behind the cylinders will be influence at a diameter of about 2-4 times the diameter of the cylinder in the direction perpendicular to the (cross) flow direction. This means that for a net, the closer the flow gets to 90° relative to the net, the more upstream twines the inflow velocity have been influenced by. For the case seen in Figure 13 the considered twine is influenced by one or possibly 2 upstream twines. Figure 16 show a case where the inflow angle approaches 90°.

As seen from Figure 16, the inflow velocity to a twine in this case is influenced by several upstream twines.

The component of the distance between two consecutive twines cross flow to the undisturbed relative velocity is $L_y \sin\Phi$ as shown in Figure 17.

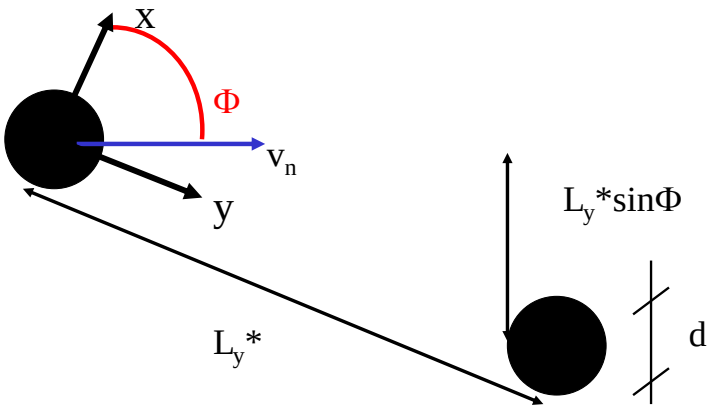

Figure 17 Definitions

It is intuitive that when $L_y^* \sin\Phi$ is lower than some K^*d where K is a factor larger than 1 depending of the width of the wake where the flow velocity is re by upstream twines. When $L_y^* \sin\Phi$ approaches 0, the drag force to the twines will be significantly reduced due to shading from upstream twines. In the special case where L_y^* is extremely much larger than d (Sn approaches 0) this effect will diminish. K may depend on several factors. In the consecutive section of this paper a value for K is proposed and compared to numerical studies. L_y^* in Figure 17 is the x-y plane distance between consecutive twines as seen in Figure 18. For non-deformed rectangular net, $L_y^* = L_y$. In a deformed state it can be lower as shown in Figure 18. All deformations including the one shown in Figure 18 is accounted for in the AquaSim analysis presented in this paper.

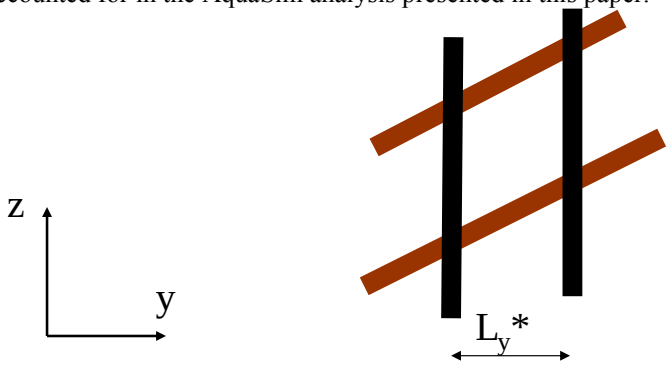

Figure 18 Definition of L_y^*

LIMITATIONS OF THE METHODOLOGY

Using the formulae presented in this paper is intended for, and useful for calculation of loads to meshes. However, the methodology has certain limitations.

The methodology assumes the fluid velocity approaching the mesh is the same as the undisturbed fluid velocity. The

presence of the mesh may introduce a global velocity field making this assumption invalid.
The methodology presented in this paper does not consider the fact that nets with the same solidity may have different drag response properties. This is seen in Tsukrov et. al. (2009). The drag properties seen in this paper focus on nylon nets which are the most commonly used in the commercial market.
The methodology does not consider the boundary layers of the flow around nets. The proposed reduction for flow at angles close to flow being parallel to the mesh is established by fit to empirical data.

COMPARISON OF ANALYSIS TO MEASUREMENTS

The net load model presented in this paper is compared to measurements by two numerical case studies. The presented load model has been introduced to AquaSim. The program is based on time domain analysis where first a current field is introduced then waves are applied. The analysis is dynamic accounting for velocities and accelerations. Both regular and irregular seas can be analysed. .
In general, AquaSim has been used to carry out analysis for a large amount of different cases where some are reported in Berstad et al. (2005a, 2005b, 2007, 2008).
The methodology described in the present paper has been introduced to AquaSim. The following parameters have been chosen:
$Cl = 0.013*Cd_{cyl}$ for M1 and M2
Cl = $0.02*Cd$ for M0 (M0-M2 described later)
$K = 2.4$
When $L_y*sin\Phi < K*d$ then Cd is scaled by

$$Cd_{mem} = Cd_{mem} * \left(\frac{Ly \sin \phi}{Kd} \right)^{1.5} \qquad (34)$$

The value for Cl has been established based on introducing realistic values to the 1/7 power law for skin friction which can be traced back to von Karman. Cl is applied to the twine circumference.

The comparison to empirical data is subdivided to two parts. First, a comparison of the proposed drag coefficient to a mesh (Cd_{mem}) from the drag coefficient to a cylinder, Cd_{cyl} is compared to empirical data by Løland (1991). Figure 19 shows a comparison between empirical data by Løland (1991) and analysis with 3 different analysis models.

- M1 is the current (from 2012) base load model in AquaSim. The model is based on Cd_{cyl} = 1.0, then Cd_{mem} is found from Equation 16. Flow parallel to the net is accounted for by Equation 31.
- M2 is the same as M1 but with Cd_{cyl} found from Figure 7.
- M0 is a model with Cd_{mem} =1.2 and no correction for inflow angle. This is the former analysis model.

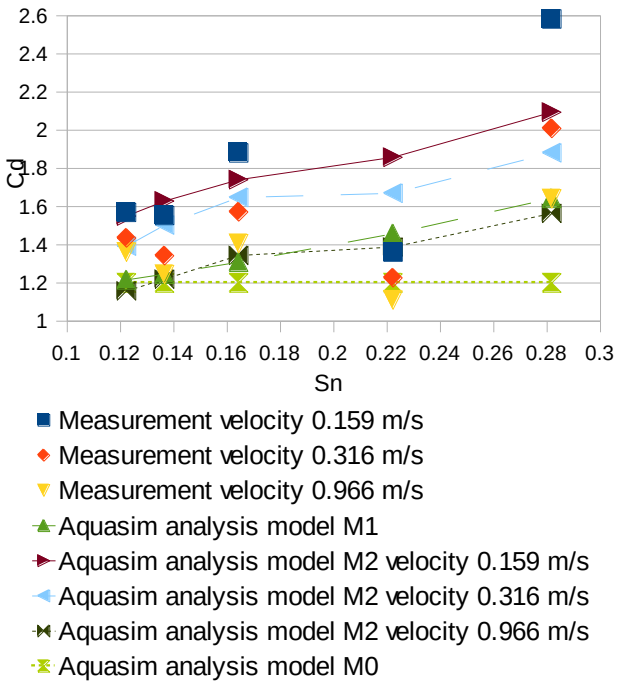

Figure 19 Comparison of analysis performed in AquaSim to measurements from Løland (1991) on a net panel

In Figure 19 the drag coefficient Cd_{mem} is plotted against the solidity ratio Sn. Measurements have been carried out for a net panel with 5 different solidities in 3 different current velocities. As seen from Figure 19 analysis and measured data compares well. At low velocity the empirical data is above the analysis at a few cases, but below for the case with solidity 22%. At high velocity empirical data and analysis corresponds very well independent whether analysis is carried out with input based on Cd from base value or from The Reynolds number consideration (M1 and M2 respectively). In NS 9415 0.5 m/s has been defined as the lower bound design criteria. Normal 50 year values for the current velocity are in the range of from 0.5 m/s to 1 m/s. Hence both M1 and M2 compare well at appropriate velocities. This shows that the chosen relation between Cd_{cyl} and Cd_{mem} is realistic for these solidity ratios.

In the second comparison, analysis has been compared to a test case presented by SFH (2010). This is a circular net without bottom as seen in Figure 20. Tests were carried out for 4 nets with key parameters given in Table 1 Tests were carried out for 7 current velocities as given in Table 2.

Table 1 Labels and key data 4 nets

Name	N19	N30	N35	N43
Length half mesh [mm]	25,5	16,2	8,3	5,8
Twine diameter [mm]	2,42	2,35	1,41	1,35
Solidity (A_e/A_{tot})	0,19	0,30	0,35	0,43
Solidity (2t/d)	0,19	0,29	0,34	0,47

.

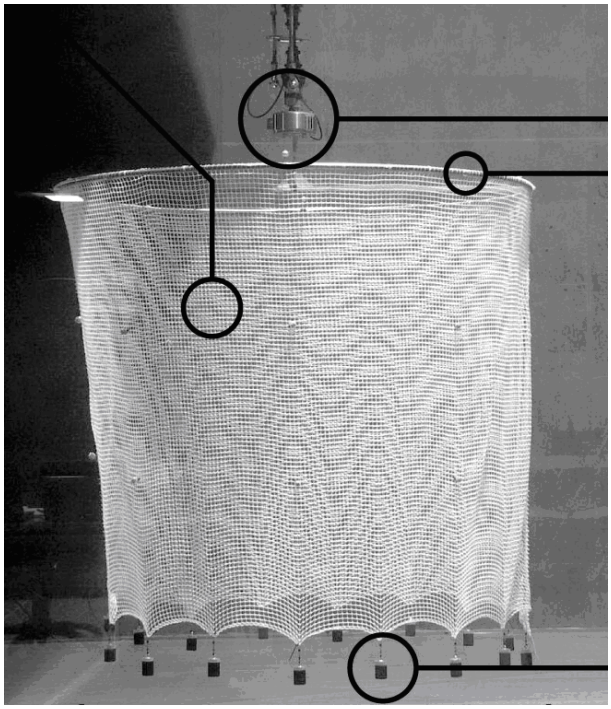

Figure 20 Test case by SFH (2010).

The cage had a diameter of 1.75 meters and the depth of the net was 1.55 m. The total force in water from bottom weights was 71.7 N. In discussion of these results the horizontal force measured on top centre of the cage is denoted the drag force whereas positive lift force is defined upwards.

Table 2 Test velocities

Test #	#1	#2	#3	#4	#5	#6	#7
Velocity[m/s]	0,13	0,25	0,37	0,50	0,63	0,75	0,90

The analysis model established in AquaSim is shown in Figure 21. The analysis model is made up by 1030 FE-elements.

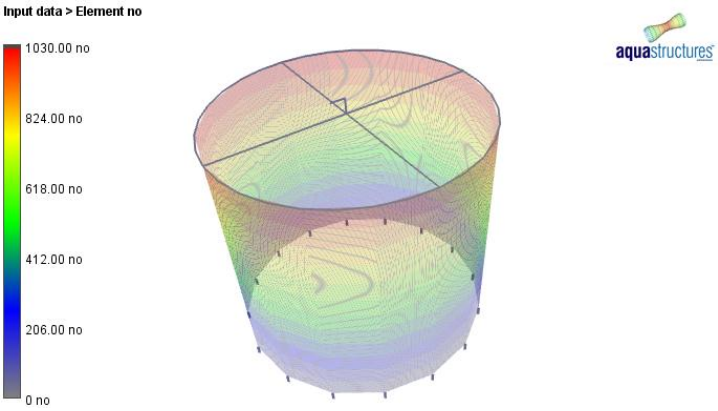

Figure 21 Analysis model of the test case

Figure 22 shows deformation of the analysis model of net N35 at a current velocity of 0.9 m/s. The analysis seen in this figure is carried out with analysis method M1.

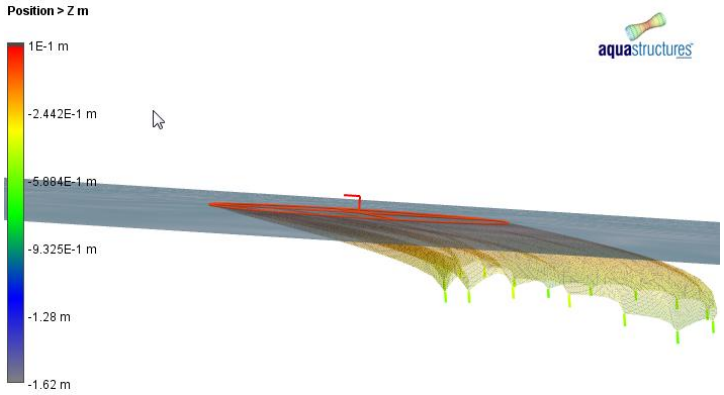

Figure 22 Deformation net N35 at 0.9 m/s

Figure 23 shows video footage of net N35 at a current velocity of 0.9 m/s. As seen by comparing to Figure 22 the deformation corresponds well between measurements and analysis.

Figure 23 Video of test case net N35 at current velocity 0.9 m/s.

Figure 24 - Figure 27 show comparisons between measurements and analysis. The abbreviations in Figure 24 - Figure 27 are explained in Table 3.

Table 3

Abbreviation	Explenation
Drag_Tank	Measured horizontal force top
Lift_Tank	Weigth at 0 velocity - vertical force, measurements
Drag_analysis	Analysed horizontal force top
Lift_analysis	Weigth at 0 velocity - vertical force, analysis

The comparison between measurements and analysis for net N19 shown in Figure 24 shows good correspondence for all analysis models except for the highest velocity where analysis model M0 estimates too high drag force. This model also estimates the lowest lift force.

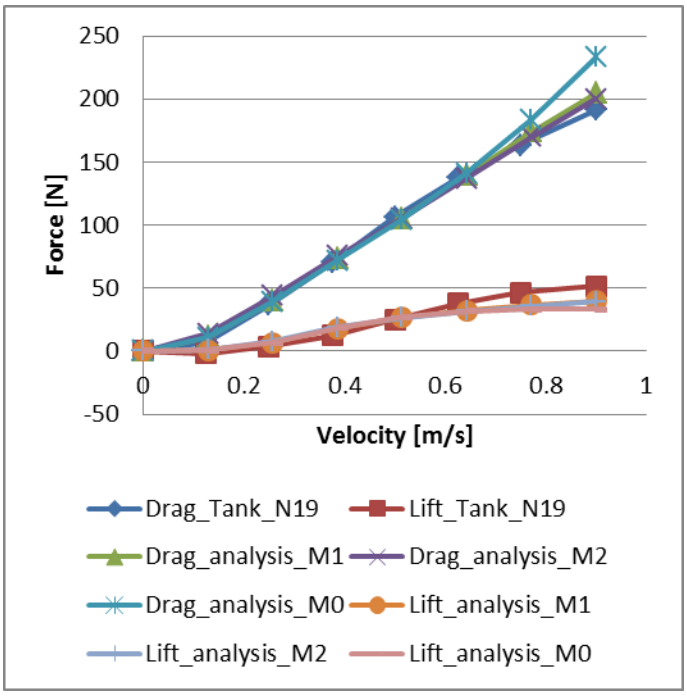

Figure 24 Net N19, solidity 19%

The results for net N30 is shown in Figure 25. Also in this case analysis model M1 and M2 shows very good agreement to measurements. The measurements have for some reason negative lift (meaning downwards) for low velocities. This is not physical and is not seen in the analysis.

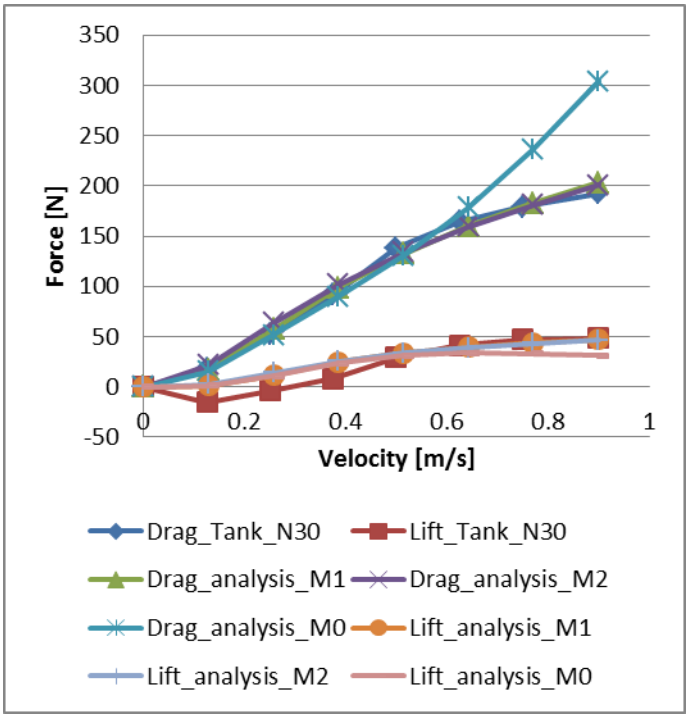

Figure 25 Net N30, solidity 30%.

Figure 26 shows results for net N35. Results compare well also for this case but not as good as for N30. The lift is in this case 76 N at velocity 0.9 m/s. This is unphysical and not seen in the analysis.

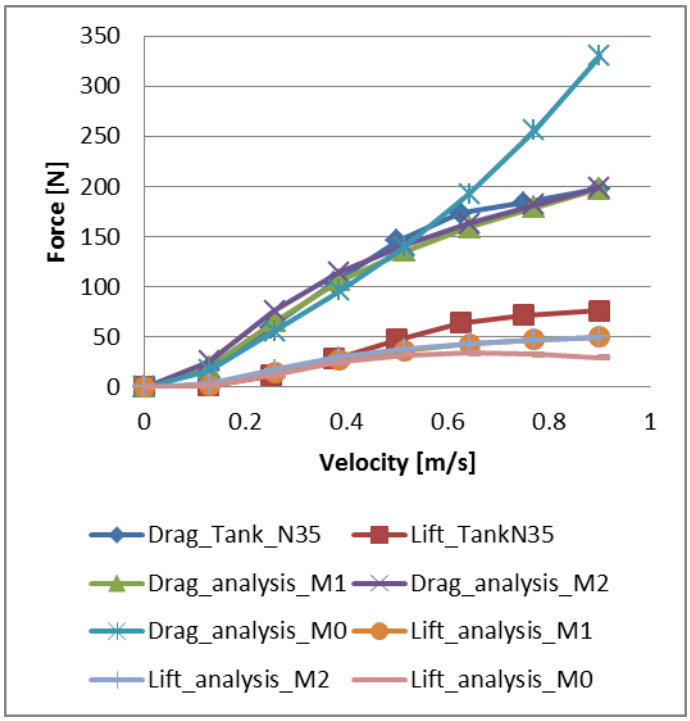

Figure 26 Net N35, solidity 35%.

The results for net N43 is seen in Figure 27. The results shows the same trend as the other results.

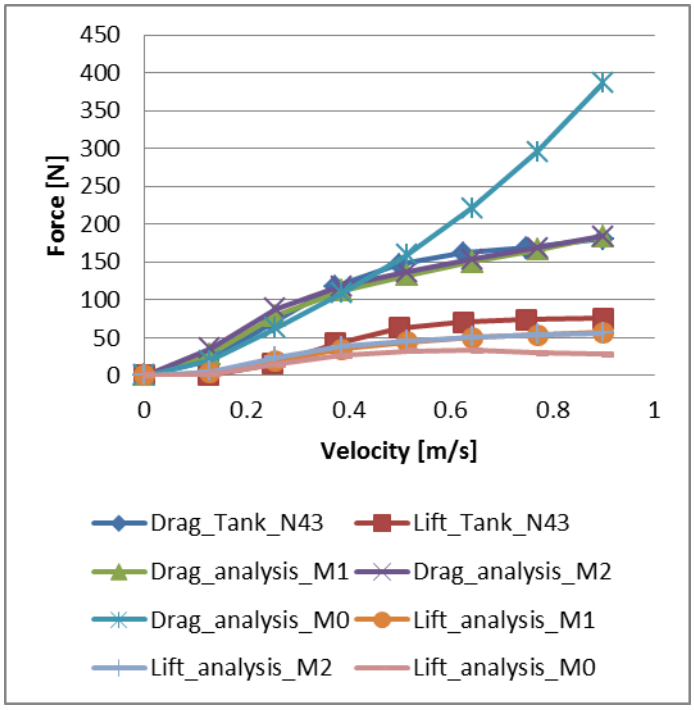

Figure 27 Net N43, solidity 43%.

From Figure 24 - Figure 27 it is seen that the analysis compare very well to measurement for drag for model M1 and M2. Model M0 turns very conservative as the net deforms. This is

because model M0 does not account for lower forces when the flow starts to become parallel to the net.

The results show that both M1 and M2 give good correspondence to test data for N19 and N30 both for drag and lift. For net N35 and N43 measured lift is a bit higher than analysis. Comparing net N30 and N35 it is seen that both measurements and analysis with model M1 and M2 give lift in the lower end of 50 N whereas measurement for N35 give 76 N and analysis 50 N. In this case there might be some errors in the measurements, or there might be some change in the physics. Also for net N35 and N43 measurements and analysis compare well for design purposes.

CONCLUSIONS

Based on testing and analysis compared to testing it can be concluded that $Cd_{mem} = Cd_{cyl} /(1-d/L)^3$ where d is twine diameter and L is the distance between consecutive twines and Cd_{cyl} is the appropriate drag coefficient for the solitary twine is introduced compares well to empirical data. A couple of other possible relations have been presented in this paper. This may be alternatives which will be more elaborated in future work.

The method presented in this paper is based on a twine by twine approach. A reduction factor based on empirical data for tangential flow is introduced. The correction factor is based on a simplified consideration of the flow pattern in the wake of cylinders. The algorithm is to introduce a reduced Cd when the inflow angle is such that a twine is in the wake of a previous twine. Results from this approach show good correspondence with empirical data.

It is concluded that to carry out the 3 step approach as done in this paper is a reasonable approach to establishing mesh loads:

1. Find an appropriate Cd for an individual twine
2. Establish an appropriate Cd for the mesh based on the Cd for the twine
3. Reduce Cd for tangential flow

Lift is derived by the cross flow principle and the 3D orientation of the lift is automatically derived. The load model described in this paper has been introduced to AquaSim which is the leading FE-analysis tool for analysis of fish farm units word wide.

The accuracy of the methodology is limited by several factors. One is the global influence on the inflow by the full net. This should be further investigated.

ACKNOWLEDGMENTS

The work has been funded by Aquastructures and the Norwegian research council, NFR. Their support is acknowledged.

REFERENCES

Aquastructures (2006a) “Benchmarking and validation of AquaSim 2006” Report no. 2006/FO-005 Aquastructures, Postboks 1223 – Pirsenteret 7462 Trondheim. www.aquastructures.no.

Aquastructures (2006b) "The AQUAstructureSIMulator. Theorethical formulation of structure and load modeling" Report No. 2006-Fo06. Aquastructures, Postboks 1223 – Pirsenteret 7462 Trondheim. www.aquastructures.no.

Balash Cheslav, Bruce Colbourne, Neil Bose, Wayne Raman (2009) "Aquaculture Net Drag Force and Added Mass" Aquacultural Engineering 41 14–21.

Barkley, D (2006) "Linear analysis of the cylinder wake mean flow" Europhys. Lett., 75 (5), pp. 750–756 (2006) DOI: 10.1209/epl/i2006-10168-7

Blevins, R.D., 1984. Applied Fluid Dynamics Handbook. Krieger Publishing Company, Florida, p. 316.

Berstad, A. J., Tronstad, H., Ytterland, A. (2004)” Design Rules for Marine Fish Farms in Norway. Calculation of the Structural Response of such Flexible Structures to Verify Structural Integrity.” Proceedings of OMAE2004 23rd International Conference on Offshore Mechanics and Arctic Engineering June 2004, Vancouver, Canada. OMAE2004-51577

Berstad, A. J. and H. Tronstad (2007) “Development and design verification of a floating tidal power unit” OMAE 2007, The 26th International Conference on Offshore Mechanics and Arctic Engineering San Diego, California, 10-15 June, 2007. Paper 29052. ISBN #: .

Berstad, A. J. and H. Tronstad (2005a) “Response from current and regular/irregular waves on a typical polyethylene fish farm”Maritime Transportation and Exploitation of Ocean and Coastal Resources. Eds. C. Guedes Soares, Y. Garbatov, N. Fonseca. 2005 Taylor & Francis Group London. ISBN #: 0 415 39036 2.

Berstad, A. J., H. Tronstad, S. A. Sivertsen and E. Leite. (2005b) “Enhancement of Design Criteria for Fish Farm Facilities Including Operations” OMAE 2005, The 24th International Conference on Offshore Mechanics and Arctic Engineering Halkidiki, Greece, 12-17 June, 2005. Paper 67451. ISBN #: 0791837599.

Darcy, H.(1856), “Les Fontaines Publiques de la Ville de Dijon” Dalmont, Paris.

Faltinsen, Odd M. (1990) “Sea loads on ships and offshore structures.” Cambridge university press ISBN 0 521 37285 2

Fredheim, Arne (2005) “Current Forces on Net Structure” Doctoral Theses at NTNU, ISSN 1503-8181; 2005:64, ISBN: 82-471-6999-1

Goldstein, S. (1965) 2Modern Developsments in Fluid Dynamics.” Dover Publications.

Kristiansen and Faltinsen (2011) “Current loads on aquaculture net cages”. Unpublished paper and oral conversation, authum 2011.

Lader, Pål F., Anna Olsen, Atle Jensen, Johan Kristian Sveen, Arne Fredheim, Birger Enerhaug (2007) "Experimental investigation of the interaction between waves and net structures—Damping mechanism" Aquacultural Engineering 37 (2007) 100–114. www.elsevier.com/locate/aqua-online.

Lader, Pål F, Tim Dempster, Arne Fredheim, Østen Jensen (2008) "Current induced net deformations in full-scale sea-cages for Atlantic salmon (Salmo salar)" Aquacultural Engineering 38 (2008) 52–65, www.elsevier.com/locate/aqua-online.

Løland, Geir (1991) “Current forces on and flow through fish farms.” Dr.Ing. Thesis, MTA-91-78. NTNU, Norwegian University of science and technology.

Morison, J. R., M.P. O'Brien, J.W. Johnson and S.A. Schaaf (1950), "The Force Exerted by Surface Waves on Piles," *Petroleum Transactions,* AIME. Vol. bold 189, 1950, 149-154.

Molin. B. (2011) “Hydrodynamic modeling of perforated structures” Applied Ocean Research 33. 1-11. Elsevier.

NS 9415(2009) Marine fish farms, Requirements for design, dimensioning, production, installations and operation. Pronorm. Postboks 252, 1326 Lysaker.

SFH (2010) “Nets with high solidity, Model testing”. Report SFH A106030. Authors: Pål Lader, Heidi Moe, Østen Jensen, Egil Lien. ISBN 9788-82-14-04946-6. Sintef Fiskeri og havbruk AS. 7465 Trondheim. www.sintef.no.

Tsukrov, I., Eroshkin, O., Fredriksson, D.W., Swift, M.R., Celikkol, B., 2003. Finiteelement modeling of net panels using a consistent net element. Ocean Engineering 30,251-270.

Tsukrov, I., Drach, A., DeCew, J.C., Swift, M.R., Celikkol, B. (2011) "Characterization of geometry and normal drag coefficients of copper nets." Ocean Engineering 38, 1979-1988.

